Dielectric Sensing using T-matched RAIN RFID Tags

Pavel Nikitin, Megan Brewster, John Kim, KVS Rao
Impinj, Seattle, WA 98109, USA, http://www.impinj.com

***Abstract*—— In this paper, we show how measurement of backscattered signal from commercial off-the-shelf RAIN (passive UHF) RFID tags attached to dielectric materials can be used for reliable measurement of dielectric properties of those materials. The method is robust, in that the tags can be generic and do not need to be specially designed or calibrated. The directly measured quantity is the frequency of backscatter (POTR) peak resonance, from which effective dielectric permittivity can be extracted. We show that it is almost independent of tag type used for measurement. Our approach can differentiate between at least four different types of dielectrics that we used in testing. One possible application of this sensing technique is identification for sorting items in recycling and sustainability use cases, such as plastics.**

I. Introduction

Minimizing, reusing, and recycling solid waste to ensure sustainable consumption and production patterns is a UN sustainable development goal [1]. Effective reuse and recycling can enable the circular economy but require accurate sortation of the post-consumer solid waste. In general, the process starts with sorting by item quality: what can be reused versus what is past end-of-life (EOL) and must be recycled. Next, recyclable items are sorted by composition to produce high purity, single composition feedstock for specific recycling processes.

However, many items slated for reuse or recycling will no longer have composition labels to enable the sortation process. For example, the label may be worn out over the item's lifetime and no longer be readable or removed by the consumer during the item's lifetime or in preparation for recycling (as many labels are not recyclable). Even if the composition label is present, in many cases it is not accurate [2] due to the complexities of open and global supply chains.

To determine item composition, sorting centers employ various methods. Near infrared (NIR) spectrometry is a common industrial method to identify the composition of recyclables such as textiles [3] and plastic [4]. However, NIR has disadvantages, such as equipment cost and inability to accurately sort items that are small or dark in color.

In 2021, nearly 30 billion passive RAIN (passive UHF) RFID tag chips were sold [5]. RAIN deployments are growing in size and number as they help to solve numerous business use cases across a variety of industries and supply chains [6]. Further, RAIN RFID promises to benefit consumers in the future with concepts such as Internet of Everything [7]. The vast majority of sold tag chips are converted into labels and attached to retail items or their packaging, constituting tagged items. A large volume and variety of recyclable items will still have an attached RFID tag at EOL [8]. Further, RAIN RFID infrastructure is cost effective and can provide item-level information beyond composition that can benefit sorters, for example authentication of items to enable their second-hand resale [9, 10]. RFID tags and integrated circuits (ICs) also need to be recycled [11-12] but this is beyond the scope of this paper.

As mentioned before, accuracy of sortation process is critical for effective recycling. RFID has been used to determine the properties of tagged items because tag performance changes depending on the dielectric it is attached to. However, all previous works (see next section) required either special custom designed tags or complicated calibrated measurement setups to allow one to determine the dielectric permittivity of the tagged item from measured tag responses.

In this paper, we show for the first time that the backscatter signal from any generic T-matched RAIN tag measured using a standard setup can be easily analyzed to detect the approximate dielectric permittivity of the item the tag is attached to, thereby enabling sortation for the reuse or recycling of the item.

II. Prior Work

While many active RF wireless technologies can be used for sensing, RFID is attractive due to its lower cost and power. In general, any RFID tags (chipless or chip-based) can be used as sensors [13]. There exist many works on using chipless RFID for sensing [14-19]. For example, [19] demonstrates how to use wideband measurement of chipless tags to deduce the dielectric permittivity of plastic items in the recycling sorting chain.

In this work, we concentrate on RAIN RFID tags which are chip-based. Sensing with chip-based RFID tags can use various approaches, there are good review publications on that topic [20]. Those approaches may include, for example, monitoring tag power state – on or off [21, 22], reading a specific tag's serialized identifier in the case of multiple tags or ICs with sensor switches placed on the object [23, 24], measuring tag antenna gain penalty [25], analyzing analog characteristics of the tag (such as minimum power to read the tag at fixed frequency [26, 27], tag resonant curve shape [28-30], backscatter signal strength or phase [31-33]), tracking a capacitance state of the impedance self-tuning circuitry in those ICs which have it [34-36] etc.

Note that UHF RFID sensing can also be based on dedicated sensors connected to the IC that has a serial interface (SPI or I2C) or to the smart tag platform that can be wirelessly- or battery- powered [37-40]. Adding batteries or rechargeable batteries to tags makes tags semi-passive (or battery-assisted), giving even more various capabilities such as more sensing intelligence at longer range. Those dedicated sensors can be used for dielectric sensing but are outside of scope of this paper.

However, all those works mentioned above required special custom designed and calibrated tag antennas, often in tandem with custom calibrated measurement setups which depended on many things such as specific IC used on the tag, etc. We propose a radically different simple measurement approach and method described in detail in the next section.

III. PROPOSED METHOD

A common antenna used in RAIN RFID tags is the well-known T-matched dipole antenna [41-43] such as one specific model [44] shown in Fig. 1 which consists of a loop coupled to a dipole. Such antenna provides a good impedance match on various items and thus is often used in ARC certified tags [45].

Fig. 1. Typical RFID tag with a T-matched antenna.

Tag performance is often characterized by threshold tag sensitivity (POTF, Power on Tag Forward) and threshold tag backscatter (POTR, Power on Tag Reverse). Those characteristics can be easily measured in any standard UHF RFID tag measurement setup. A typical threshold backscatter power response of a T-matched tag is shown in Fig. 2. The resonant frequency f_{potr} defines the location of the POTR peak.

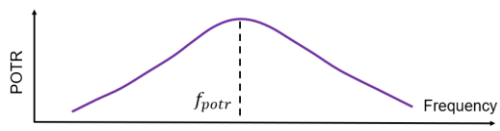

Fig. 2. Threshold POTR of a typical T-matched tag.

The antenna impedance of a T-matched dipole can be approximated by a transformer-based circuit (or its equivalent inductor representation) familiar to many researchers which we will not replicate here. In [46], it was derived using circuit theory that the threshold POTR of T-matched tags reaches maximum value at the frequency $\omega_{potr} = 2\pi f_{potr}$:

$$\omega_{potr}^2 = \frac{\omega_1^2}{1-k^2} \ , \tag{1}$$

where $\omega_1 = 2\pi f_1$ is the natural resonant frequency of a dipole portion of the tag, or basically a frequency at which the tag antenna resistance peaks. In (1), k is the coupling coefficient between the dipole and the loop ($0<k<1$). One can see from (1) that unlike POTF resonances (see formulas for those also in [46]), ω_{potr} does not depend at all on neither chip capacitance nor loop inductance.

Natural resonance of printed dipole antenna depends on antenna geometry and the properties and size of dielectric slab it is attached to. As a result, POTR peak resonance shifts down in frequency when the tag is placed on a dielectric. However, the coupling between the loop and the dipole in T-matched tags is magnetic and does not change. That makes the frequency of POTR peak an easily measurable marker, excellent for tracking the change in natural resonant frequency ω_1 of a tag antenna on dielectrics. This frequency can be related to the POTR peak frequency in free space via the effective permittivity ε_{eff} of an equivalent infinite dielectric surrounding the tag antenna, which scales the POTR resonance frequency as:

$$f_{potr}^{mat} = \frac{f_{potr}^{vacuum}}{\sqrt{\varepsilon_{eff}}} \ , \tag{2}$$

From (2), the relative POTR peak shift can be related to the effective dielectric permittivity as:

$$\varepsilon_{eff} = \frac{1}{(1-\Delta)^2}, \text{ where } \Delta = \frac{f_{potr}^{vacuum} - f_{potr}^{mat}}{f_{potr}^{vacuum}} \ . \tag{3}$$

Assume that RFID tag metal antenna is placed directly on the slab of dielectric material of finite size and thickness as shown in Fig. 3. There exist several works that propose approximate formulas for calculating the effective permittivity for printed dipoles [47-49]. Those formulas were used in some subsequent works for dielectric sensing using generic antennas [50-52], for RFID tag design optimized for specific dielectrics [53-54] and even attempts to use change in RFID tag read range as an indicator of dielectric permittivity [55-57].

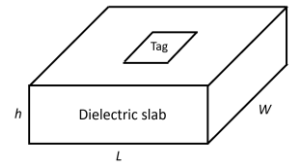

Fig. 3. Tag on dielectric slab

For example, [48] gives a well-known formula for effective permittivity of a flat dipole antenna on a substrate:

$$\varepsilon_{eff} = 1 + \left(\frac{\varepsilon-1}{2}\right)\frac{K_2}{K_1} \ , \tag{4}$$

where K_1 and K_2 are dependent on the properties and the size of a dielectric slab the antenna is placed on as well as on the geometry of the antenna itself.

In the next section we empirically demonstrate that effective dielectric permittivity calculated using eq. (3) is very similar for different T-matched tags with different shapes and sizes of antennas. That means that it is sufficient to monitor only the relative shift of f_{potr} (compared to its free space value) for any tag to determine the dielectric permittivity of the item another tag is attached to. Any tags (the more the better, of course) can be used for producing a calibration curve that relates the effective permittivity (calculated from relative POTR peak shift) to the actual permittivity of the tagged material.

Note that the frequency of the POTR peak location is easy to measure reliably and using any standard wideband RFID test equipment such as Voyantic Tagformance [58] or CISC RAIN RFID Xplorer [59]. For example, a Gen2 Query measurement with Voyantic (5 MHz frequency step and 0.1 dB power step) takes about 30 seconds across 500 MHz of bandwidth. It also does not matter how exactly RSSI is defined (definitions between readers and various measurement equipment can vary by a few dB's, depending on which backscatter spectral harmonics are counted), what is the distance to the tag, how the tag is oriented relative to reader antenna, etc. - as long as the measurement is performed in far field. Also note that the POTR peak frequency is independent of several other factors such as the type of tag IC (its impedance and sensitivity), the parasitic capacitance and resistive losses in the direct-die IC attachment, whether the IC has self-tuning impedance matching capability (and whether it is enabled or disabled), etc.

To summarize, in our proposed method, we measure the relative shift of the POTR peak, calculate effective permittivity, and then empirically correlate it to the actual dielectric permittivity of the specific dielectric slab. That correlation (calibration) needs to be done only once for dielectric slabs of a certain size and thickness and applies to any type of tags.

IV. Measurements

We measured ten types of tags (listed in Table I) on four dielectric slabs (listed in Table II) in our anechoic chamber setup shown in Fig. 4 with Voyantic Tagformance. Most tags were dry inlays. Tags were tested flat on slabs from the edge direction. Tags had various sizes, antenna geometries, and several generations of various RFID ICs, from Impinj Monza 4 and Monza 5 to Monza R6 and the Impinj M700 series [60].

TABLE I. Tags tested

Tag	Size (mm)	IC	Image
Taking Things TT-422	42x16	Impinj M730	
Invengo Bullet	42x16	Impinj M730	
Arizon AZ-E53	44x18	Impinj Monza 5	
LAB ID UH424	50x30	Impinj Monza 4	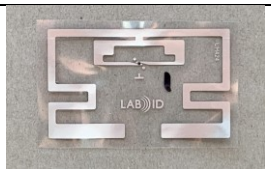
SML GB1	50x30	Impinj Monza 5	
Avery Dennison AD-381	50x30	Impinj Monza 5	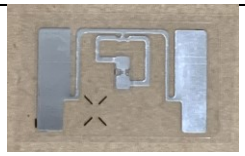
Beontag H61	50x30	Impinj Monza R6	
Beontag E62	70x14	Impinj Monza R6	
Arizon AZ-HR7	70x14	Impinj M730	
Paragon ID PID 70x14 Explorer	70x14	Impinj M730	

Fig. 4. Our measurement setup

TABLE II. Dielectric materials used

Material	Size (mm)	Dielectric permittivity @ 1.1 GHz	Dielectric loss tangent @ 1.1 GHz	Image
PTFE	130x130 x4	2.05	0.0002	
PVC	130x130 x4	3.00	0.0079	
FR4	130x130 x3.2	4.87	0.0141	
Rubber	130x130 x4	6.73	0.0247	

All tags were attached to the dielectric slabs with antenna side facing down as shown in Fig. 5 using clear Scotch Magic tape which had negligible effect on the results of testing on our 3.2-4 mm thick dielectric slabs.

Fig. 5. Examples of tag attachment using clear tape, with antenna side and chip facing the dielectric: H61 on FR4 and PID 70x14 on PTFE.

The measurements on tags with Monza R6 and M700 ICs were done with Impinj AutoTune function both enabled and disabled - it did not have any effect on the POTR peak frequency. Typical measured POTF and POTR curves for one of the tags (AD-381) are shown in Fig. 6.

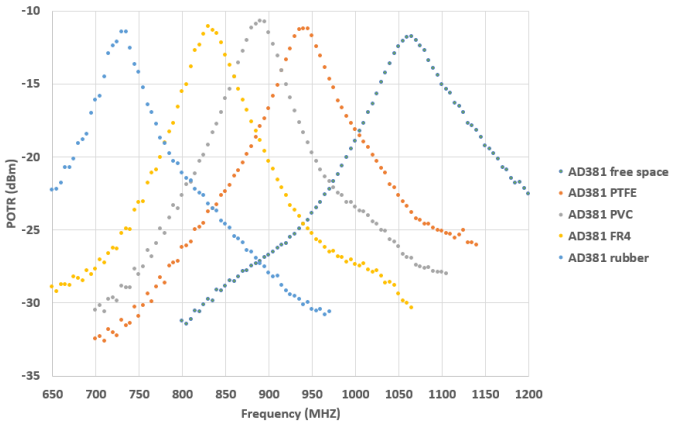

Fig. 6. Measured threshold POTR responses of AD-381 on dielectrics.

Note that we used commercially produced tags, some of which were certified by ARC [45] which has strict quality requirements. Sample-to-sample variation still exists but is quite small as one can see from Fig. 7 which shows ten samples of PID 70x14, randomly sampled from the roll containing 500 inlays and measured both in free space and on PTFE material.

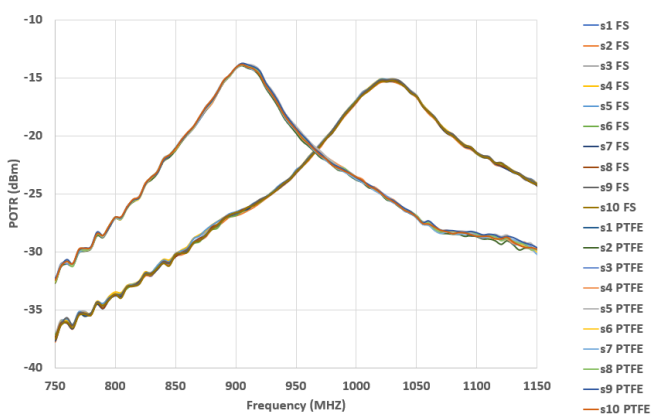

Fig. 7. POTR of ten PID 70x14 tag samples (labeled S1 through S10) in free space (FS) and on PTFE

Indeed, POTR peak frequency is very robust and easily measurable marker for resonant frequency shift measurement because it is independent of IC impedance, sensitivity, or parasitic IC mounting capacitance.

V. Results and Analysis

Table III shows the POTR peak frequencies for all measured tags on all dielectric slabs (we used a 5 MHz step, so the accuracy of locating peak frequency was about 2.5 MHz).

We plotted in Fig. 8 the effective dielectric permittivity calculated using eq. (3) as a function of the actual slab permittivity. As one can see, different tags, with different shapes of antennas, behave very similarly.

TABLE III. Frequency of POTR peak (MHz)

	Free space	PTFE	PVC	FR4	RUBBER
Tag \ Eps	**1**	**2.05**	**3**	**4.87**	**6.73**
TT422	1037.5	900	840	770	667.5
Bullet	1025	887.5	825	760	660
AZ-E53	1022.5	887.5	827.5	760	655
UH424	957.5	837.5	782.5	720	630
SML GB1	980	860	810	750	665
AD-381	1065	940	885	830	730
H61	975	862.5	815	752.5	652.5
AZ-HR7	997.5	887.5	840	785	695
E62	1035	920	870	800	700
PID 70x14	1025	905	845	792.5	702.5

To understand that, recall that all the tags we used have T-matched printed dipole antennas where metal arms thickness (~0.01 mm) is substantially smaller than the source feed gap between the arms (~0.15 mm), which is much smaller than the dielectric slab thickness (4 mm), which in turn is much smaller than the overall electrical length of each tag antenna (>10 cm). Because of those relations (we refer our readers to [48] for more details), the effective dielectric permittivity dependence on specific geometry of the tag antenna is weak.

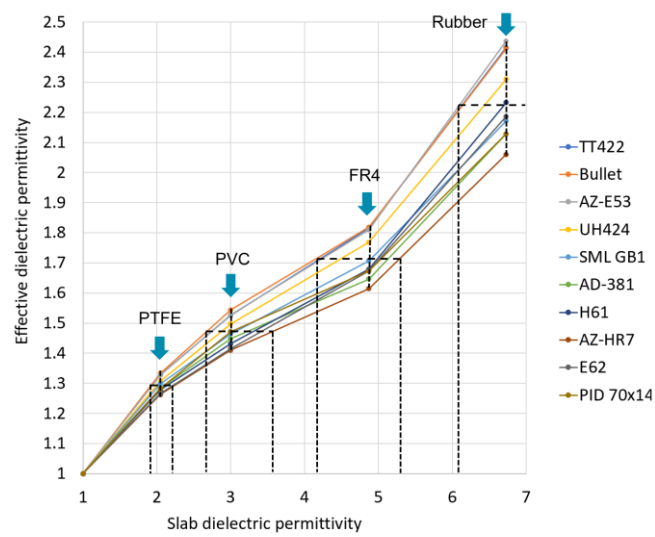

Fig. 8. Effective dielectric permittivity vs. actual slab permittivity.

Of course, there exists data spread between different tags, and it grows as dielectric permittivity increases, as Fig. 8 also clearly shows. The data spread would result in a certain error in determining actual material permittivity. We estimate the accuracy of our method to be about 15% for dielectrics with permittivity 5 or less (see spread bounds in Fig. 8). However, as Table IV demonstrates, in our tag population the standard deviation of effective permittivity is only about 6% even in the case of a heavy dielectric material (rubber).

TABLE IV. Effective permittivity for measured tags

	PTFE $\varepsilon = 2.05$	PVC $\varepsilon = 3$	FR4 $\varepsilon = 4.87$	RUBBER $\varepsilon = 6.73$
ε_{eff}	1.297	1.473	1.721	2.248
St. dev. of ε_{eff}	0.0264	0.0483	0.0761	0.1368

VI. Discussion and Future Work

The described method is certainly dependent on the size and thickness of the dielectric material which affects the effective dielectric permittivity and hence the tag dipole resonance which we measure by determining POTR peak frequency. This dependence needs to be further studied.

One interesting question is how tag antennas other than T-matched dipoles (for example, nested-slot type antennas described in [42]) would perform in this method.

Another interesting research question is minimizing the number of test points in frequency domain. For faster testing, fewer points are desired. Both Voyantic Tagformance and CISC RAIN RFID Xplorer already include algorithms for using only a few points for fast tag production testing. Perhaps, a good polynomial approximation can be applied to reconstruct POTR peak from the limited number of test points and then determine its resonant frequency.

Also, changes in the absolute POTR peak value can potentially be analyzed to characterize material tangent loss.

One should keep in mind that since this method requires broadband transmission in far field, in order to comply with spectrum regulations it would most likely have to be used in laboratory setting or shielded environment.

VII. Applications

As we mentioned before, one potential application of this method is plastics identification for sorting tagged items in a recycling chain. Fig. 9 shows an envisioned process of sensing to determine material composition. Assume that all tagged items use plastic of the same thickness. Wideband equipment measures the POTR response for each tag, finds the peak frequency and compares it to the peak frequency for the same tag in free space. Then effective permittivity is calculated, which is then related to actual permittivity via a previously made calibration curve, similar to the one in Fig. 8. Based on that, a sorting decision is made in real time.

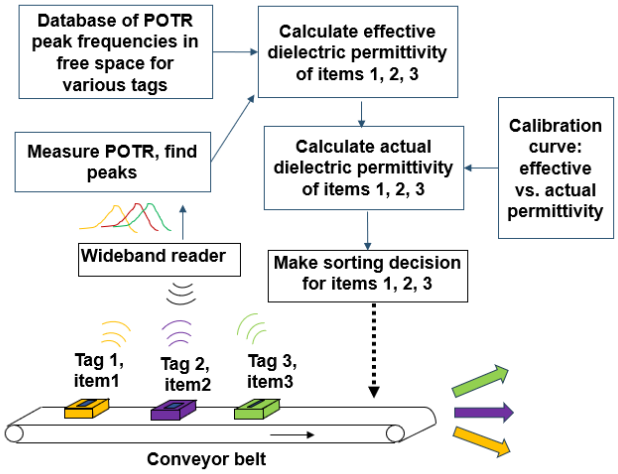

Fig. 9. Envisioned application: sensing process for plastics identification during sorting tagged items in recycling chain.

The POTR peak frequency in free space for each tag can be stored in a cloud database or even in the memory of the tag itself (storing an integer frequency value up to 2048 MHz would require only 12 bits of memory).

One other potential application that follows from the method's dependence on dielectric thickness can actually be determining the thickness of the dielectric objects. This is something that near infrared spectrometry cannot easily do.

VIII. Conclusions

In this paper, we proposed a simple method to measure the dielectric permittivity of tagged items from measured tag backscatter, regardless of specific T-matched dipole tags used (any ICs and any antenna geometries).

The method is based on measuring POTR peak frequency shift relative to free space, calculating an effective dielectric permittivity, and then finding the actual dielectric permittivity via a calibration curve. The method is dependent on the size and thickness of the dielectric material, but the calibration curve is almost independent of the tag used, as long as tags are T-matched flat dipoles.

One application that we envision is quick plastics identification for sorting tagged items in a recycling chain in real time.

References

[1] Transforming our world: the 2030 Agenda for Sustainable Development https://sdgs.un.org/2030agenda

[2] Clothing labels: accurate or not? https://www.circle-economy.com/resources/clothing-labels-accurate-or-not

[3] K. Cura et al., "Textile Recognition and Sorting for Recycling at an Automated Line Using Near Infrared Spectroscopy", MDPI Jpurnal of Polymer Recycling, February 2021

[4] V. Lahtela, T. Karki, "Mechanical Sorting Processing of Waste Material Before Composite Manufacturing – A Review", Journal of Engineering Science and Technology Review, December 2018, pp. 35-46

[5] RAIN RFID Tag IC 2021 Sales Hit 30 Billion https://rainrfid.org/rain-rfid-tag-ic-2021-sales-hit-30-billion/

[6] RAIN RFID market research report https://rainrfid.org/rain-rfid-market-research-report/

[7] IEEE CRFID and RAIN Alliance: HeroX challenge – Resolving the Internet of Every Thing, https://www.herox.com/digitaltwins/teams

[8] O. Ondemir, M. A. Ilgin and S. M. Gupta, "Optimal End-of-Life Management in Closed-Loop Supply Chains Using RFID and Sensors," in IEEE Trans. on Industrial Informatics, vol. 8, no. 3, pp. 719-728, 2012

[9] I. Bose and S. Yan, "The Green Potential of RFID Projects: A Case-Based Analysis," in IT Professional, vol. 13, no. 1, pp. 41-47, Jan.-Feb. 2011

[10] H. Schindler et al., "Smart Trash: Study on RFID tags and the recycling industry" RAND technical report TR-1283-EC, 2012: https://www.rand.org/pubs/technical_reports/TR1283.html

[11] P. Krauchi, P. A. Wager, M. Eugster, G. Grossmann and L. Hilty, "End-of-life impacts of pervasive computing," in IEEE Technology and Society Magazine, vol. 24, no. 1, pp. 45-53, 2005

[12] Y. Zhang and U. Guin, "End-to-End Traceability of ICs in Component Supply Chain for Fighting Against Recycling," in IEEE Transactions on Information Forensics and Security, vol. 15, pp. 767-775, 2020

[13] B. S. Cook et al., "RFID-Based Sensors for Zero-Power Autonomous Wireless Sensor Networks," in IEEE Sensors Journal, vol. 14, Aug. 2014

[14] S. Tedjini, N. Karmakar, E. Perret, A. Vena, R. Koswatta and R. E-Azim, "Hold the Chips: Chipless Technology, an Alternative Technique for RFID," in IEEE Microwave Magazine, vol. 14, no. 5, pp. 56-65, 2013

[15] S. Dey, J. K. Saha and N. C. Karmakar, "Smart Sensing: Chipless RFID Solutions for the Internet of Everything," in IEEE Microwave Magazine, vol. 16, no. 10, pp. 26-39, 2015

[16] P. Fathi, N. C. Karmakar, M. Bhattacharya and S. Bhattacharya, "Potential Chipless RFID Sensors for Food Packaging Applications: A Review," IEEE Sensors Journal, vol. 20, no. 17, pp. 9618-9636, 2020

[17] S. R. Patre, "Passive Chipless RFID Sensors: Concept to Applications—A Review," in IEEE Journal of RFID, vol. 6, pp. 64-76, 2022

[18] A. Subrahmannian and S. K. Behera, "Chipless RFID: A Unique Technology for Mankind," IEEE Journal of RFID, vol. 6, 2022

[19] F. Villa-Gonzalez, R. Bhattacharyya and S. Sarma, "Single and bulk identification of plastics in the recycling chain using Chipless RFID tags," IEEE International Conference on RFID, Atlanta, 2021, pp. 1-8

[20] F. Costa et al., "A Review of RFID Sensors, the New Frontier of Internet of Things", Sensors, vol.21, no.9, pp.3138, 2021

[21] M. Philipose, J. R. Smith, B. Jiang, A. Mamishev, S. Roy and K. Sundara-Rajan, "Battery-free wireless identification and sensing," IEEE Pervasive Computing, vol. 4, no. 1, pp. 37-45, Jan.-March 2005

[22] R. Bhattacharyya, C. Floerkemeier and S. Sarma, "RFID tag antenna based sensing: Does your beverage glass need a refill?," IEEE International Conference on RFID, Orlando, FL, USA, 2010, pp. 126-133

[23] L. Catarinucci, R. Colella and L. Tarricone, "A Cost-Effective UHF RFID Tag for Transmission of Generic Sensor Data in Wireless Sensor Networks," in IEEE Trans. on MTT, vol. 57, no. 5, pp. 1291-1296, 2009

[24] G. Marrocco, "Pervasive electromagnetics: sensing paradigms by passive RFID technology," in IEEE Wireless Communications, vol. 17, 2010

[25] J. D. Griffin, G. D. Durgin, A. Haldi and B. Kippelen, "RF Tag Antenna Performance on Various Materials Using Radio Link Budgets," in IEEE Antennas and Wireless Propagation Letters, vol. 5, pp. 247-250, 2006

[26] J. Siden, X. Zeng, T. Unander, A. Koptyug and H. -E. Nilsson, "Remote Moisture Sensing utilizing Ordinary RFID Tags," IEEE SENSORS Conference, Atlanta, GA, USA, 2007, pp. 308-311

[27] R. Bhattacharyya, C. Floerkemeier and S. Sarma, "Low-Cost, Ubiquitous RFID-Tag-Antenna-Based Sensing," in Proceedings of the IEEE, vol. 98, no. 9, pp. 1593-1600, 2010

[28] J. Virtanen et al., "Inkjet-Printed Humidity Sensor for Passive UHF RFID Systems," in IEEE Transactions on Instrumentation and Measurement, vol. 60, no. 8, pp. 2768-2777, Aug. 2011

[29] S. Capdevila, L. Jofre, J. Romeu and J. C. Bolomey, "Multi-Loaded Modulated Scatterer Technique for Sensing Applications," in IEEE Trans. on Instrumentation and Measurement, vol. 62, no. 4, pp. 794-805, 2013

[30] H. Lobato-Morales, A. Corona-Chávez, J. L. Olvera-Cervantes, R. A. Chávez-Pérez and J. L. Medina-Monroy, "Wireless Sensing of Complex Dielectric Permittivity of Liquids Based on the RFID," in IEEE Transactions on Microwave Theory and Techniques, vol. 62, no. 9, pp. 2160-2167, Sept. 2014

[31] C. Occhiuzzi, S. Caizzone and G. Marrocco, "Passive UHF RFID antennas for sensing applications: Principles, methods, and classifcations," in IEEE Antennas and Propagation Magazine, vol. 55, no. 6, pp. 14-34, Dec. 2013

[32] X. Wang, J. Zhang, Z. Yu, S. Mao, S. C. G. Periaswamy and J. Patton, "On Remote Temperature Sensing Using Commercial UHF RFID Tags," in IEEE Internet of Things Journal, vol. 6, no. 6, pp. 10715-10727, Dec. 2019

[33] J. Lejarreta-Andrés, J. Melià-Seguí, R. Bhattacharyya, X. Vilajosana and S. E. Sarma, "Toward Low-Cost RF-Based Bulk Fabric Classification for the Textile Industry," in IEEE Sensors Journal, vol. 22, no. 16, 2022

[34] M. C. Caccami and G. Marrocco, "Electromagnetic Modeling of Self-Tuning RFID Sensor Antennas in Linear and Nonlinear Regimes," in IEEE Trans. on Antennas and Propagation, vol. 66, no. 6, June 2018

[35] X. Zhang, H. -X. Li and H. S. -H. Chung, "Setup-Independent UHF RFID Sensing Technique Using Multidimensional Differential Measurement," IEEE Internet of Things Journal, vol. 8, no. 13, pp. 10509-10517, 1 2021

[36] F. Nanni, S. Nappi and G. Marrocco, "Potentiometric Sensing by means of Self-tuning RFID ICs," IEEE RFID Conference, 2022

[37] A. P. Sample, D. J. Yeager, P. S. Powledge, A. V. Mamishev and J. R. Smith, "Design of an RFID-Based Battery-Free Programmable Sensing Platform," in IEEE Transactions on Instrumentation and Measurement, vol. 57, no. 11, pp. 2608-2615, Nov. 2008

[38] S. J. Thomas, E. Wheeler, J. Teizer and M. S. Reynolds, "Quadrature Amplitude Modulated Backscatter in Passive and Semipassive UHF RFID Systems," in IEEE Transactions on Microwave Theory and Techniques, vol. 60, no. 4, pp. 1175-1182, April 2012

[39] D. De Donno, L. Catarinucci and L. Tarricone, "RAMSES: RFID Augmented Module for Smart Environmental Sensing," in IEEE Trans. on IE, vol. 63, no. 7, pp. 1701-1708, July 2014

[40] S. J. Thomas, "RFID for Everyone: Design of an Easily-Accessible, Experimental UHF RFID Platform," IEEE RFID Conference, 2019

[41] Son H-W, Pyo C-S. "Design of RFID tag antennas using an inductively coupled feed", Electronics Letters, 2005, 41(18):994–992

[42] G. Marrocco, "The art of UHF RFID antenna design: impedance-matching and size-reduction techniques," in IEEE Antennas and Propagation Magazine, vol. 50, no. 1, pp. 66-79, Feb. 2008

[43] D. D. Deavours, "Analysis and design of wideband passive UHF RFID tags using a circuit model," IEEE RFID Conference, 2009, pp. 283-290

[44] Beontag E62 RFID tag: https://www.atlasrfidstore.com/beontag-e62-rfid-paper-tag-monza-r6-p/

[45] ARC Program at Auburn University: https://rfid.auburn.edu/arc/

[46] P. Nikitin, J. Kim and K. Rao, "RFID Tag Analysis Using an Equivalent Circuit," 2021 IEEE International Symposium on Antennas and Propagation and USNC-URSI Radio Science Meeting (APS/URSI), Singapore, Singapore, 2021, pp. 167-168

[47] D. Jackson and N. Alexopoulos, "Analysis of planar strip geometries in a substrate-superstrate configuration," in IEEE Transactions on Antennas and Propagation, vol. 34, no. 12, pp. 1430-1438, December 1986

[48] A. Abbosh, "Accurate Effective Permittivity Calculation of Printed Center-Fed Dipoles and Its Application to Quasi Yagi-Uda Antennas," in IEEE Trans. on Ant. and Prop., vol. 61, no. 4, pp. 2297-2300, April 2013

[49] Kanesan, Theele, Kiefe, "A Robust Method of Calculating the Effective Length of a Conductive Strip on an Ungrounded Dielectric Substrate", PIERS 2014

[50] G. Castorina, L. Di Donato, A. F. Morabito, T. Isernia and G. Sorbello, "Analysis and Design of a Concrete Embedded Antenna for Wireless Monitoring Applications [Antenna Applications Corner]," in IEEE Antennas and Propagation Magazine, vol. 58, no. 6, pp. 76-93, Dec. 2016

[51] A. Abdelnour, A. Rennane, D. Kaddour and S. Tedjini, "Non-destructive dielectric characterization method for food products," 2017 IEEE MTT-S International Microwave Symposium (IMS), 2017, pp. 2022-2024

[52] H. Saghlatoon, R. Mirzavand, P. Mousavi, "Fixed-Frequency Low-Loss Dielectric Material Sensing Transmitter", IEEE Transactions on Industrial Electronics, vol.68, no.4, pp.3517-3526, 2021

[53] L. A. Kosuru and D. D. Deavours, "Optimum performance for RFID tag immersed in dielectric media," IEEE RFID Conference, 2011

[54] S. Shao, R. J. Burkholder and J. L. Volakis, "Design Approach for Robust UHF RFID Tag Antennas Mounted on a Plurality of Dielectric Surfaces," in IEEE Antennas and Propagation Magazine, vol. 56, no. 5, pp. 158-166, Oct. 2014

[55] Y. Chenwei and G. Wang, "UHF RFID tag sensitive to object material," 2015 Loughborough Antennas & Propagation Conference (LAPC), Loughborough, UK, 2015, pp. 1-3

[56] C. Yang, Y. Tao, H. Man and W. Zhu, "Dielectric Sensing-aid Structure for RFID Tag," 2019 IEEE International Conference on RFID Technology and Applications (RFID-TA), Pisa, Italy, 2019, pp. 248-251

[57] Y. Chen, C. Hua and Z. Shen, "Circularly Polarized UHF RFID Tag Antenna for Wireless Sensing of Complex Permittivity of Liquids," in IEEE Sensors Journal, vol. 21, no. 23, pp. 26746-26754, 1 Dec.1, 2021

[58] Voyantic Tagformance Pro: https://voyantic.com/lab/tagformance-pro/

[59] CISC RAIN RFID Xplorer: https://www.cisc.at/product/rain-rfid-xplorer/

[60] M700 series IC: https://www.impinj.com/products/tag-chips